Recep Tayyip Erdoğan Üniversitesi Fen ve Mühendislik Bilimleri Dergisi, 2(2) 83-104 2021
Recep Tayyip Erdogan University Journal of Science and Engineering, 2(2) 83-104 2021
ISSN: 2687-2315 / E-ISSN: 2757-7686

Impacts of Collector Radius and Height on Performance Parameters of Solar Chimney Power Plants: A Case Study for Manzanares, Spain

Harun SEN[1,2], Pinar Mert CUCE[2,3], Erdem CUCE[1,2*]

[1] Department of Mechanical Engineering, Faculty of Engineering and Architecture, Recep Tayyip Erdogan University, Zihni Derin Campus, 53100 Rize, Turkey
[2] Low/Zero Carbon Energy Technologies Laboratory, Faculty of Engineering and Architecture, Recep Tayyip Erdogan University, Zihni Derin Campus, 53100 Rize, Turkey
[3] Department of Architecture, Faculty of Engineering and Architecture, Recep Tayyip Erdogan University, Zihni Derin Campus, 53100 Rize, Turkey

[*]Sorumlu Yazar/Corresponding Author
E-mail: erdem.cuce@erdogan.edu.tr
Orcid ID: 0000-0003-0150-4705

Araştırma Makalesi/Research Article
Geliş Tarihi/Received: 02.11.2021
Kabul Tarihi/Accepted: 29.11.2021

ABSTRACT

In this study, based on the Manzanares prototype, a typical SCPP system is considered with a collector height of 1.85 m, a chimney with a height of 194.6 m and a diameter of 10.16 m, and a collector with a radius of 122 m. With the 3D CFD model designed in ANSYS, the impacts of the change in the collector radius and collector height on the system performance are analysed by considering the turbulence effects. The numerical results are compared with the experimental data on the power output capacity of the pilot plant at different radiant fluxes and a good agreement is obtained. Then, by taking the chimney height and diameter constant, the numerical solutions are repeated for different collector radii in the range of 52.5-175 m. The results indicate that increasing the collector area, which means increasing the energy entering the system, leads to a notable improvement in the power output of the pilot plant. With a collector radius of 175 m, a power output of 95 kW can be obtained whereas it is 55 kW in the reference case with a collector radius of 122 m. Similarly, the solutions are repeated by changing the collector height between 1.1 and 4 m while keeping the other dimensions constant. It is seen that the increase in collector height negatively affects the performance of the system. It is observed that reducing the collector height to 1.1 m for the pilot plant can increase the power output to 61.77 kW.

Keywords: Solar chimney power plants, Collector radius, Collector height, Power output, System efficiency, CFD

Toplayıcı Yarıçapı ve Yüksekliğinin Güneş Bacası Güç Santrallerinin Performans Parametreleri Üzerine Etkileri: Manzanares, İspanya için Bir Vaka Çalışması

ÖZET

Manzanares prototipinin esas alındığı bu çalışmada 1.85 m kolektör yüksekliği, 194.6 m yüksekliğinde ve 10.16 m çapında bacası ve 122 m yarıçapında kolektörü olan tipik bir GBGS sistemi göz önünde bulundurulur. ANSYS'te tasarlanan 3 boyutlu HAD modeli ile türbülans etkilerini göz önünde bulundurarak kollektör yarıçapı ve kollektör yüksekliğinde meydana gelecek değişikliğin sistem performansına olan etkileri analiz edilir. Sayısal sonuçlar pilot tesisin farklı ışınım akılarında güç çıkış kapasitesi deneysel verilerle karşılaştırılır ve iyi bir uyum sağlanır. Daha sonra baca yüksekliği ve çapı sabit alınarak 52.5-175 m aralığında farklı kollektör yarıçapları için sayısal çözümler tekrarlanır. Sonuçlar, sisteme giren enerjinin artması anlamına gelen kollektör alanının arttırılmasının, pilot tesisin güç çıkışında kayda değer bir iyileşmeye yol açtığını göstermektedir. 175 m kollektör yarıçapı ile 95 kW güç çıkışı elde edilebilirken, 122 m kollektör yarıçapı ile referans durumda 55 kW güç çıkışı elde edilebilir. Benzer şekilde diğer ölçüler sabit tutularak kollektör yüksekliği 1.1 ile 4 m arasında değiştirilmek suretiyle çözümler tekrarlanır. Kollektör yüksekliğindeki artışın sistemin performansını olumsuz etkilediği görülür. Pilot tesis için kollektör yüksekliğini 1.1 m'ye düşürmenin güç çıkışını 61.77 kW'a çıkartabileceği gözlemlenir.

Anahtar Kelimeler: Güneş bacası güç santralleri, Kollektör yarıçapı, Kollektör yüksekliği, Güç çıkışı, Sistem verimi, HAD

Cite as;
Sen, H., Cuce, P.M., Cuce, E. (2021). Impacts of Collector Radius and Height on Performance Parameters of Solar Chimney Power Plants: A Case Study for Manzanares, Spain, *Recep Tayyip Erdogan University Journal of Science and Engineering*, 2(2), 83-104. Doi: 10.53501/rteufemud.1017909

1. Introduction

Today, the majority of the energy demand in the world is supplied in the form of conversion of fossil fuels into heat energy. The increasing human population and the unequivocal rise in energy need have increased the use of fossil fuels, which has brought environmental pollution and CO_2 emissions to an irresistible level. This situation has stimulated scientists to focus more on clean and renewable energy technologies. Renewable energy sources, which are the source of clean energy, have become the centre of interest because they do not pollute the nature and do not emit CO_2. Solar energy is one of the most popular clean energy sources with its current potential. This popularity of course comes from efficient and well-established systems developed to harness solar thermal and electrical power. Solar electricity has shown an outstanding progress over the last 50 years notably photovoltaics (PVs). Parameter extraction and feasibility models for PV systems work flawlessly (Cuce and Bali, 2009), and the installation capacity of PV applications shows a rising trend every year. However, even PVs are criticised today because they do not allow electricity production during the hours when the incoming solar energy is limited or not available. At this point, solar chimney power plants (SCPPs) are becoming a focus of attention as they can produce electricity continuously regardless of environmental conditions (Sen and Cuce, 2020). SCPP systems basically consist of 3 parts; which are the collector, the chimney and the turbine fixed in the chimney. The solar radiation received into the system through the collector is transmitted to the ground due to the semi-transparent feature of the collector. The incoming solar radiation transmitted to the ground causes an increase in temperature here. Since the temperature on the ground is warmer than the system air under the collector, there is a heat transfer from the ground to the system air. During this heat transfer, the system air, whose temperature increases, moves upwards due to the density difference and heads towards the chimney, which is the only outlet point of the system. A long chimney in the centre of the collector creates a pressure difference, and the system air whose temperature increases is forced upwards from the chimney ground due to this pressure difference. The system air, whose thermal energy content is enhanced, leaves the system by increasing its velocity in the chimney (Cuce and Cuce, 2019a). Kinetic energy of air is improved as a consequence of the rise in temperature and velocity values, and then this energy is converted into electrical energy by means of the turbine located at a specific height in the chimney. What makes SCPPs special is that the pressure difference created by the high chimney continues even during the absence of the sun, allowing electricity generation for 24 hours (Schlaich et al., 2005).

Although studies on SCPPs have shown a rising trend in recent years, the concept dates back to early 1900s. The idea of generating electricity with a SCPP was first put forward by Spanish engineer Isodoro Cabanyes in 1903 (Dhahri and Omri, 2013). However, the implementation of the first prototype takes place in the 1980s. Haaf et al. (1983) states that the first prototype, built in 1982 in Manzanares, Spain, has a 194.6 m high and 10.08 m diameter chimney, has a 122 m semi-permeable plastic collector, and the average height of this collector is 1.85 m. He also states that there is a turbine with 4 blades and a radius of 5 m with 83% efficiency, positioned 9 m above the ground in the chimney. Later, Haaf (1984) emphasises that the ideal power output of the system is 48 kW based on the experimental measurements, the temperature increase of the system reaches 20°C during the day, and the maximum air velocity in the chimney is 20 m/s. In following works, the researchers analyse the effects of environmental and geometric parameters on SCPP systems with mathematical, theoretical and CFD studies based on experimental results. Mullet (1987) emphasises that the height of the chimney should reach 1000 m in order for the overall efficiency of the system to exceed 1%. Pasumarthi and Sherif (1998a) investigate the performance parameters of SCPP systems by a theoretical approach.

Later, they demonstrate the validity of the theoretical model with their experimental work (Pasumarthi and Sherif, 1998b). Zhou et al. (2007) carry out an experimental study to examine the performance of SCPP systems and to predict the performance of different systems by developing a mathematical model. They make measurements using a chimney made of PVC pipe with a diameter of 0.35 m and a height of 1 m and a collector made of glass and plastic with a radius ranging from 1 to 5 m. They underline that increasing the collector radius in the simulations performed with the experimental data enhances the power output of the system.

It is difficult to test the impacts of climatic and geometric parameters on SCPP systems experimentally, which leads researchers to more mathematical, theoretical and CFD studies, especially for large-scale systems. Tayebi et al. (2018) analyse the pressure, temperature and velocity distributions across the collector of the Manzanares prototype at different solar intensities with the 3D CFD model they developed. They report that the increase in solar intensity will improve the temperature rise in the collector, the pressure difference and the air velocity. Al Alawin et al. (2012) simulate the power output estimation of a SCPP plant planned to be built in Jordan, and evaluate the effect of chimney height on the system through mathematical software. They claim that for a SCPP system with 3.5 m chimney and 40 m collector diameter, the power output will be 60 kW when the chimney height is 50 m, and the power output will be 30% more when the chimney height is 210 m. Similarly, they show that the efficiency of the system would increase approximately 4 times to 0.66%. The researchers also analyse the effects of different geometrical changes on the system parameters such as power output, air flow rate, efficiency, temperature rise, etc. (Toghraie et al., 2018; Dhahri et al., 2014; Shahi et al., 2018; Cuce and Cuce, 2019b).

It is seen that the parameters affecting the performance of SCPPs have been studied many times in the literature. It is possible to collect these studies under two headings as climatic and geometric parameters in general. Researchers investigating the impacts of climatic parameters on the system interpret the effect of changes in ambient temperature and solar intensity on the air movement in the system (Cuce et al., 2020a; Dhahri et al., 2014; Toghraie et al., 2018). Although climatic data are region-specific, they are parameters that cannot be interfered with from the outside. The effects that increase the performance of a typical SCPP are possible with more design parameters. For this reason, it is seen that researchers aim to increase the performance of the system by constructing different designs with geometric parameters. The most common of these parameters is the height of the chimney. The chimney is the driving force of the system. For this reason, it is expected that the chimney to be designed higher will increase the power output. In the recent works, which reference the Manzanares pilot plant, researchers claim that increasing the height of the chimney will increase the power output of the system (Cuce et al., 2020b; Zhou et al., 2009; Ayadi et al., 2018).

Another parameter that directly affects the performance of the system, such as the chimney height, is the collector radius. Researchers underline that increasing the collector radius will increase the energy entering the system and in this case, it will increase the power output (Daimallah et al., 2020; Li et al., 2012; Yapıcı et al., 2020). The design of the elements of the system is as important as their size. Researchers claim that if the chimney of the system is vertical, divergent and convergent, it will give different results (Yapıcı et al., 2020; Nasraoui et al., 2020; Bouabidi et al., 2018; Xu and Zhou, 2018; Dewangan, 2021; Das and Chandramohan, 2020). In particular, some researchers argue that the system with a divergent chimney structure will give higher power output than other chimney designs (Cuce et al., 2021a; Hassan et al., 2018; Hu et al., 2017). Like the chimney design, the collector is also an important parameter affecting the system. Researchers evaluate the effect of the collector with different

inclination angles on the system (Hoseini and Mehdipour, 2018; Setareh, 2021; Hassan et al., 2018). It is claimed by the researchers that the collector slope increases the power output of the system but will decrease it after a point (Ahirwar and Sharma, 2019; Keshari et al., 2021). Another design parameter that affects the system is the ground. Since the slope that can be made on the ground will support the upward movement of the air in the system, it can create a performance improvement (Cuce et al., 2020c; Cuce et al., 2021b).

In SCPP systems, the part that uses solar energy is the collector. In this study, the effect of collector radius and height on the system will be examined. Since the increase in the collector radius will increase the area where the solar energy is transferred to the system, there is an expectation that the performance of the system will improve. Since a higher positioned collector will increase the amount of air entering the system, it is expected to increase the air flow rate in the system, but this increase may affect the temperature rise of air in the plant. With the study, the impacts of the changes in the collector height and radius of the Manzanares pilot plant on the outputs of the system are analysed and discussed.

2. Materials and Method

The goal of the study is to analyse the influence of collector radius and height of a SCPP system on the performance figures. A high-accuracy analysis is aimed, taking into account the geometric dimensions and material properties of the pilot plant. For this reason, the model created is first verified with the power output of the pilot plant for a solar intensity range of 200-1000 W/m^2. Assuming that there is no change in climatic conditions after verification, the conservation and turbulence equations are solved simultaneously for steady-state conditions and simulations are performed. The heat losses in the chimney are neglected and the Boussinesq approximation is considered appropriate for the density since the temperature change in the system is low. The flow through the system is assumed to be turbulent, and the radiation equation is followed by a discrete coordinate (DO) non-gray radiation model. The equations in the solution are as follows (ANSYS Inc, 2016):

- Continuity equation:

$$\frac{\partial(\rho u)}{\partial x}+\frac{\partial(\rho v)}{\partial y}+\frac{\partial(\partial w)}{\partial z}=0 \quad \textbf{(1)}$$

- Momentum equation:

$$\frac{\partial(\rho uu)}{\partial x}+\frac{\partial(\rho uv)}{\partial y}+\frac{\partial(\rho uw)}{\partial z}=-\frac{\partial p}{\partial x}+\mu\left(\frac{\partial^2 u}{\partial x^2}+\frac{\partial^2 u}{\partial y^2}+\frac{\partial^2 u}{\partial z^2}\right) \quad \textbf{(2)}$$

$$\frac{\partial(\rho vu)}{\partial x}+\frac{\partial(\rho vv)}{\partial y}+\frac{\partial(\rho vw)}{\partial z}=-\frac{\partial p}{\partial y}+\mu\left(\frac{\partial^2 v}{\partial x^2}+\frac{\partial^2 v}{\partial y^2}+\frac{\partial^2 v}{\partial z^2}\right) \quad \textbf{(3)}$$

$$\frac{\partial(\rho wu)}{\partial x}+\frac{\partial(\rho wv)}{\partial y}+\frac{\partial(\rho ww)}{\partial z}=-\frac{\partial p}{\partial z}+\mu\left(\frac{\partial^2 w}{\partial x^2}+\frac{\partial^2 w}{\partial y^2}+\frac{\partial^2 w}{\partial z^2}\right)+\rho g\beta(T-T_a) \quad \textbf{(4)}$$

- Energy equation:

$$\frac{\partial(pcuT)}{\partial x}+\frac{\partial(pcvT)}{\partial y}+\frac{\partial(pcwT)}{\partial z}=\lambda\left(\frac{\partial^2 T}{\partial x^2}+\frac{\partial^2 T}{\partial y^2}+\frac{\partial^2 T}{\partial z^2}\right) \quad \textbf{(5)}$$

In SCPP systems, there is natural convection from the entrance of the air to the collector and up to the chimney outlet. Dimensionless Rayleigh number for natural convection is as follows:

$$Ra=\frac{g\beta\Delta T H_c{}^3}{\alpha v} \quad \textbf{(6)}$$

In equation (6), α is the thermal diffusion coefficient, ν is the kinematic viscosity, H_c is the collector height from ground, and g is the acceleration of gravity. The critical value of Ra number for transition to turbulence is 10^9. In this study, the entire flow is considered turbulent since the Ra number is greater than the critical Ra value (Zandian and Ashjaee, 2013). As the turbulence model, the RNG k-ε turbulence model, which gives more successful results in

eddy effects, is preferred and its equation is as follows (Abdelmohimen and Algarni, 2018; ANSYS Inc, 2016):

$$\frac{\partial}{\partial x_i}(\rho k u_i) = \frac{\partial}{\partial x_j}\left[\alpha_k \mu_{eff} \frac{\partial k}{\partial x_j}\right] + G_k + G_b + \rho\varepsilon - Y_M + S_k \quad \textbf{(7)}$$

$$\frac{\partial}{\partial x_i}(\rho \varepsilon u_i) = \frac{\partial}{\partial x_j}\left[\alpha_\varepsilon \mu_{eff} \frac{\partial \varepsilon}{\partial x_j}\right] + C_{1_\varepsilon}\frac{\varepsilon}{k}(G_k + C_{3\varepsilon}G_b) - C_{2\varepsilon}\rho\frac{\varepsilon^2}{k} - R_e + S_\varepsilon \quad \textbf{(8)}$$

Since the density variation in the system is small, the Boussinesq approximation is appropriate and the following equation is given for the density:

$$(\rho - \rho_a)g \approx -\rho_a \beta (T - T_a) g \quad \textbf{(9)}$$

In the equation (9), ρ_α is the density of the initial air, T_α is the temperature of the initial air, and β is the coefficient of thermal expansion. The energy entering the system is thermal energy and it is through the collector. It can be given by the following equation:

$$\dot{Q} = \dot{m} C_p \Delta T \quad \textbf{(10)}$$

Here, $\dot{Q}$ is the energy entering the system through the collector, $\dot{m}$ is the mass flow rate of the system air, C_p is the specific heat capacity of the air, and ΔT is the temperature difference of air from collector inlet to outlet. The collector efficiency is directly related to the solar intensity entering the system and the collector area, and can be given as follows:

$$\eta_{coll} = \frac{\dot{Q}}{A_{coll} G} \quad \textbf{(11)}$$

A_{coll} in the equation (11) is the collector area, and G indicates the amount of solar intensity. The power output of the system depends on the volumetric flow rate Q_v, the turbine pressure drop ΔP_t, and the turbine efficiency η_t:

$$P_o = \eta_t \Delta P_t Q_v \quad \textbf{(12)}$$

Although the turbine efficiency is taken differently by the researchers, its range is 75-90%. In the conducted study, the turbine efficiency is taken as 80% (Abdelmohimen and Algarni, 2018). Researchers have different uses for turbine pressure drop. While some researchers express the turbine pressure drop as a function of the air flow rate across the turbine (Guo et al., 2014), some researchers use a constant turbine pressure drop ratio (Dai et al., 2003; Nizetic et al., 2008; Kashiwa and Kashiwa, 2008). In this study, a constant turbine pressure drop ratio (r_t = 2/3) is taken. The turbine pressure drop can be calculated through:

$$\Delta P_t = r_t P_t \quad \textbf{(13)}$$

P_t in the equation (13) is the relative pressure difference where the turbine is located and is taken from the CFD results. The efficiency of the system is a measure of how much of the total energy entering the system is converted into electricity, and is calculated by:

$$\eta = \frac{P_o}{A_{coll} G} \quad \textbf{(14)}$$

In the study carried out, the 3D planar symmetric CFD model references the geometric dimensions of the Manzanares prototype in Spain. The geometric dimensions of the pilot plant are given in Table 1. In addition, the material properties are taken in accordance with the prototype, and the details about the collector, chimney and ground are given in Table 2. The prototype ground, which is a natural storage material, is based on sandstone (dos Santos Bernardes et al., 2009). The schematic and boundary conditions of the system are shown in Figure 1a. In CFD analysis, 90° models with 2 planar symmetry planes (XZ and YZ) are created in terms of economy. The design and mesh images are shown in Figure 1b. The collector inlet as well as the chimney outlet is open to the atmosphere, and the pressure difference is equal to 0 at the inlet and outlet. The solar radiation angle falling on the collector is calculated automatically with 13 hours of sunshine on June 21, by entering the coordinates of Manzanares, Spain as -3.37 longitude, 38.99 latitude and local time GM +2 by means of a solar calculator using the Discrete Ordinates (DO) solar ray tracing method via ANSYS FLUENT (Cuce et al., 2020b). As a

turbulence model, the RNG k-ε turbulence model is applied to the solution by considering the wall function and full buoyancy effects. The applied CFD details are given in Table 3. The resolutions are done with pressure-velocity binding. By choosing SIMPLE as the layout, the Green Gauss Cell Based effect is taken into account in all solutions. PRESTO is used for pressure and second order upwind analysis is used in all cases. With the hybrid initialisation, all analyses are performed with 1000 W/m^2 constant solar intensity and 293.15 K constant ambient temperature. Solutions take about 5 – 25 hours between 3000 – 4000 iterations.

Table 1. Main dimension of the Manzanares prototype (Haaf et al., 1983)

Parameter	Value
Average collector radius	52.5 – 175 m
Average collector height	1.1 – 4 m
Chimney height	194.6m
Chimney radius	5.08m
Ground thickness	0.5m

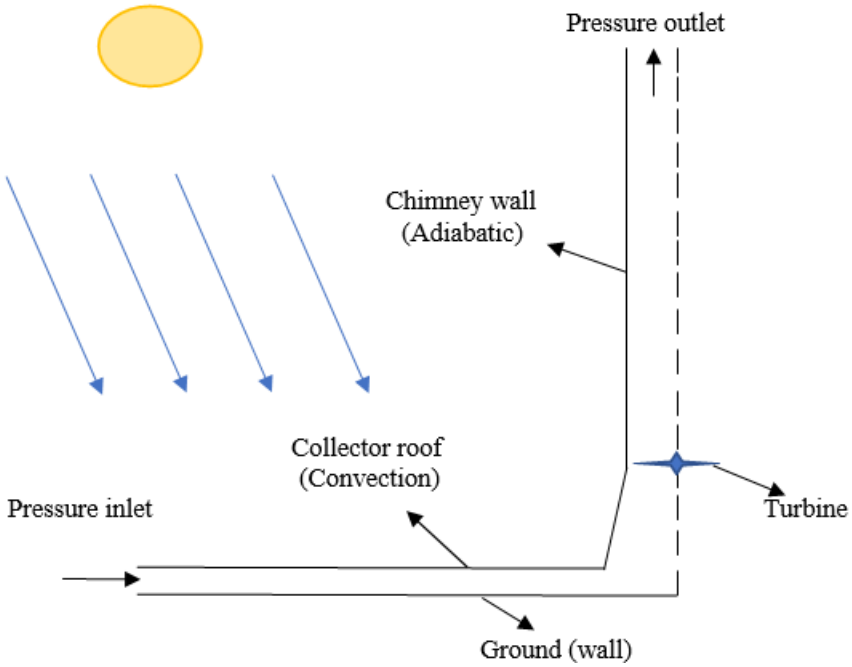

Figure 1. (a) Structural details and boundary conditions considered in the CFD research

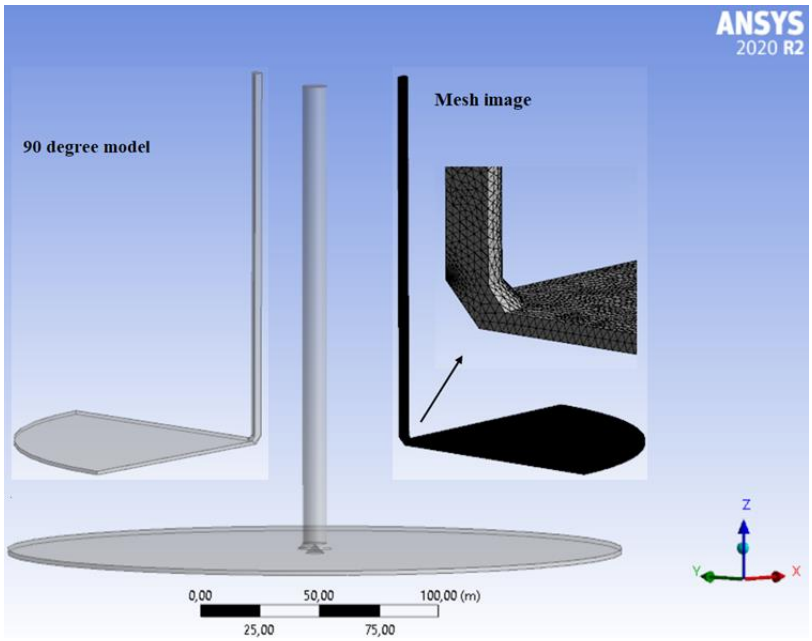

Figure 1. (b) 90 degree model and mesh images

Table 2. Details of material properties used in CFD (Cuce et al., 2020b)

Characteristic feature	Collector	Ground	Chimney
Density (kg.m^{-3})	2.50×10^{3}	2.16×10^{3}	2.719×10^{3}
Thermal cond. (W.m^{-1}K^{-1})	11.5×10^{-1}	18.3×10^{-1}	2.024×10^{2}
Specific heat (J.kg^{-1}K^{-1})	0.75×10^{3}	0.71×10^{3}	0.871×10^{3}
Absorption coeff.	0.03	0.9	0
Transmissivity	0.9	Opaque	Opaque
Emissivity	0.1	0.9	1
Refractive index	1.526	1	1
Thickness (m)	0.004	0.5	0.00125

Table 3. Parameters used in CFD model analysis. (Cuce et al., 2020b)

Solar intensity (W.m^{-2})	10^{3}
Air pressure (Pa)	101325
Ambient temperature (K)	293.15
Gravitational acceleration (m.s^{-2})	9.81
Ambient air density (kg.m^{-3})	1.2046
Ideal gas constant (J.kg^{-1}K^{-1})	287
Thermal conductivity of air (W.m^{-1}K^{-1})	0.0259
Kin. viscosity of air (m^{2}.s^{-1})	14.8×10^{-6}
Heat capacity of air (J.kg^{-1}K^{-1})	1.006×10^{3}
Stefan-Boltzmann constant (W.m^{-2}K^{-4})	5.667×10^{-8}
Pressure drop ratio in turbine	2/3

3. Results and Discussion

When examining the impacts of collector radius and height on the system performance, mesh-independent solution is required before the CFD simulations. For the mesh-independent solution, the maximum air flow rate (V_m) in the system is analysed through 3 different cell counts. Comparative results are given in Table 4. For the number of cells 388177 (for the 90° model), it is seen that the % change of the maximum air flow rate in the system compared to the number of cells of 310576 is 0.518 only. This change is quite sufficient when compared to other studies in the literature. All CFD analyses are performed on a minimum number of 388177 cells.

Table 4. Mesh-independent solution results for the CFD analyses

Cell Amount	Max. velocity (m/s)	% Change in velocity	Solution time (h)
258385	14.03790	-	3.06
310576	14.12960	0.653	4.05
388177	14.20285	0.518	5.23

In all analyses, 1000 W/m^2 constant solar intensity and 293.15 K ambient temperature are taken as reference. To confirm the accuracy of the generated CFD model, the power outputs of the Manzanares pilot plant at solar intensities of 0-1000 W/m^2 are compared with the experimental data at the aforesaid reference values. Comparative graph of CFD results and experimental data is given in Figure 2. After it is seen that the results are quite consistent, the collector radius and height of the pilot plant are changed and the potential impacts on the system performance are interpreted. The system behaviour is examined by keeping the collector height constant at 1.85 m and changing the collector radius between 52-175 m. Then, the collector radius is fixed as 122 m and the collector height is changed between 1.1-4 m, and the effect on the system is observed. The collector is the unit where solar energy is transferred to the system. For this reason, increasing the radius increases the energy entering the system, resulting in a direct performance enhancement. In Figure 3, the air velocity distribution in the system is given for 3 different values of the collector radius. In the image, it is understood from the findings that the air flow rate increases with the collector radius.

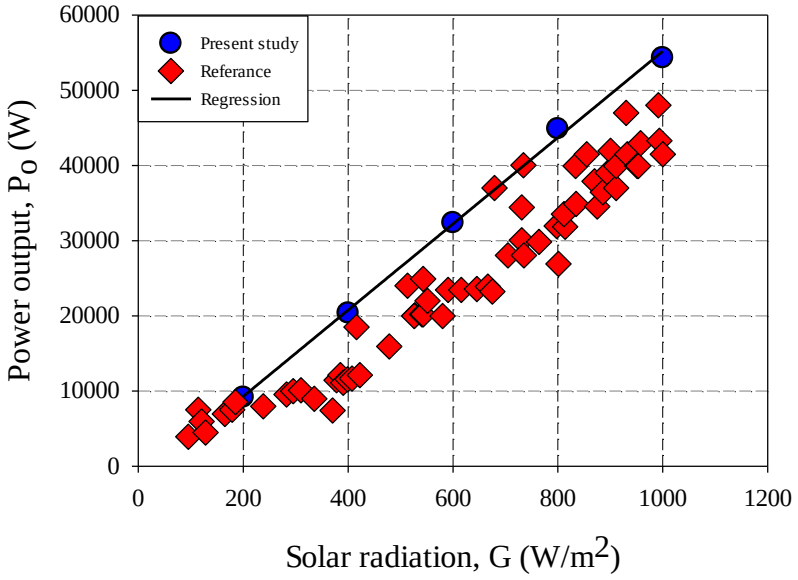

Figure 2. Power output comparison from experimental data and CFD results

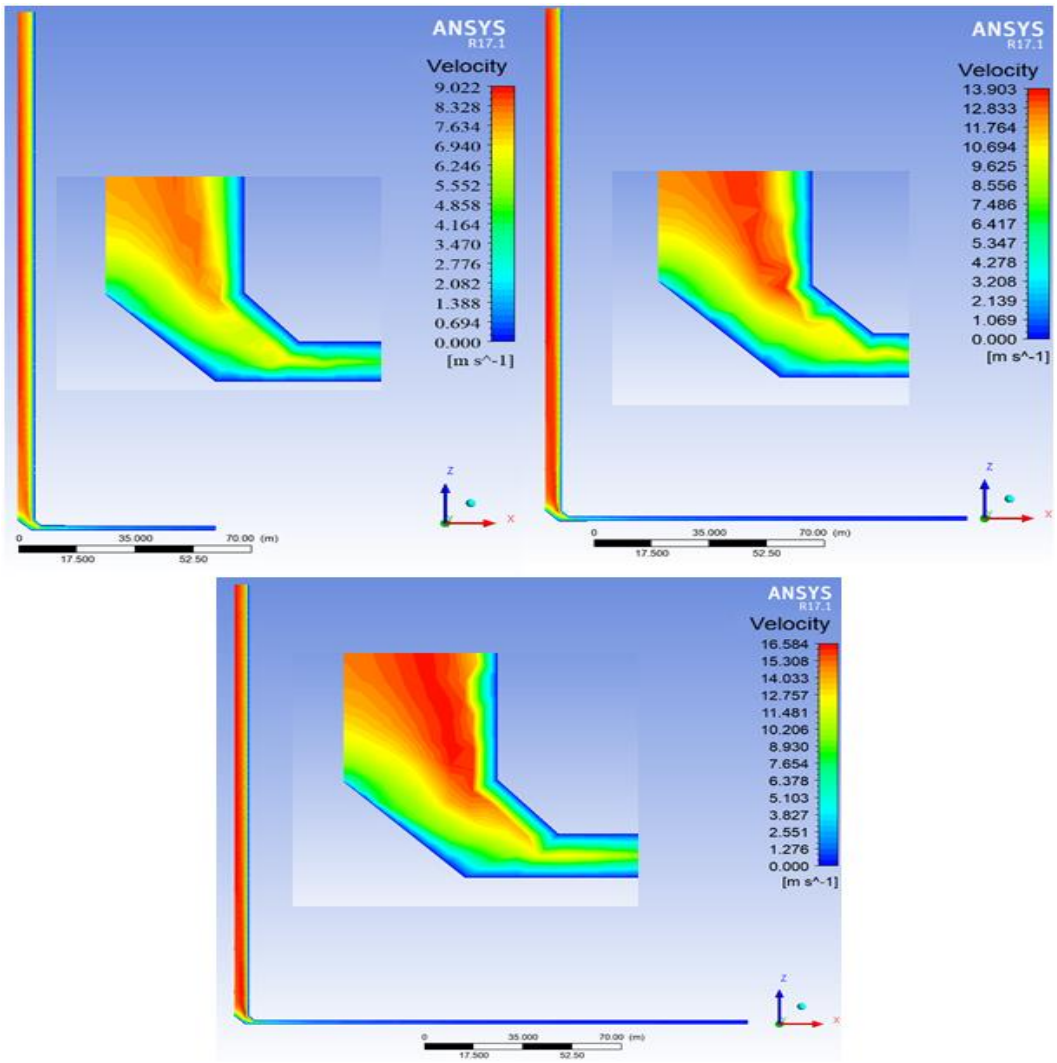

Figure 3. Velocity contours for 52.5, 122 and 175 m collector radius

Since the collector radius is the main parameter that determines the total energy entering the system, its effects on the system behaviour are very clear. At a constant ambient temperature of 293.5 K, the increase in the collector radius is expected to affect the temperature rise in the system. The impact of the change in collector radius on the temperature rise of air in the system is given in Figure 4. When the temperature increase of the air under the collector is examined, it is seen that it rises with the increase of the collector radius. The regression of the graph is an indication that the energy entering the system increases linearly with the collector radius. Theoretically, the increase in the collector radius increases the collector area, in this case the energy entering the system also increases linearly. The temperature rise corresponding to different collector radii can be calculated by the following equation:

$$\Delta T = -0.8128 + 0.1395 R_{coll} \quad \textbf{(15)}$$

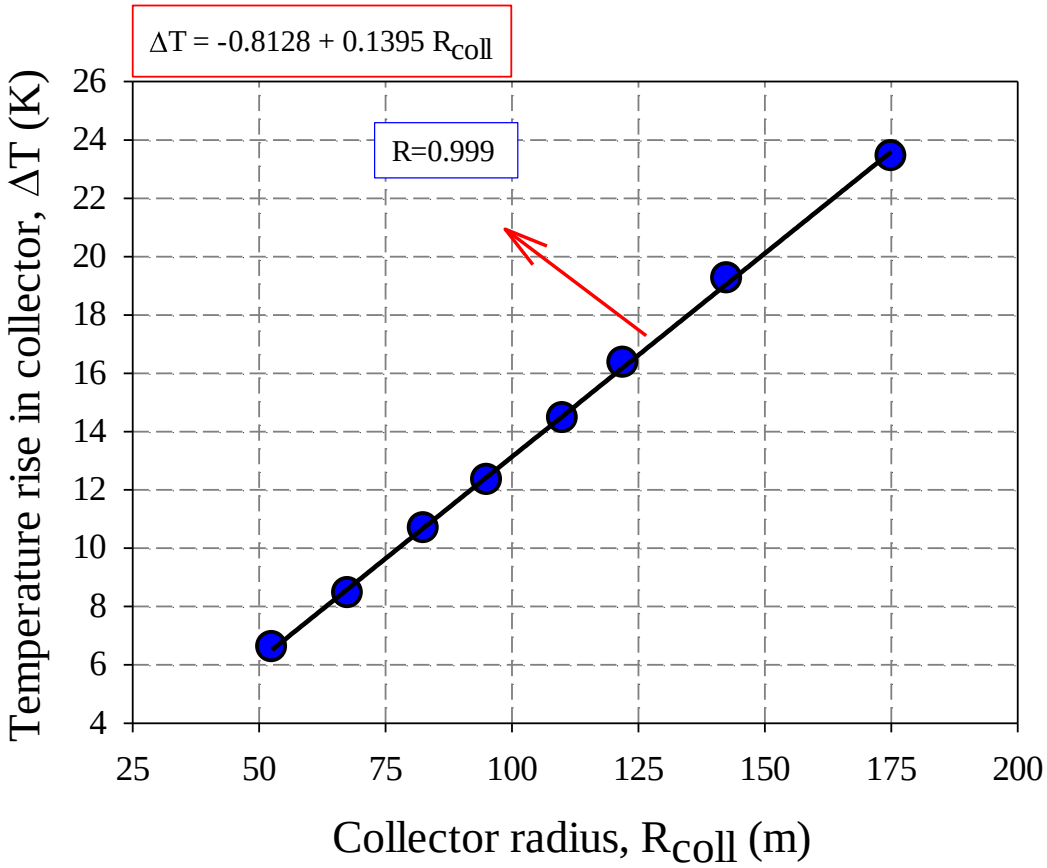

Figure 4. The temperature rise under the collector with the collector radius

It is explained that the collector radius increases the temperature rise in the system. It is expected that the temperature increase in the system will increase the kinetic energy of the system air under the collector and naturally increase the air flow rate. It is seen that the maximum air velocity, which is approximately 14.2 m/s with a collector radius of 122 m in the reference case, decreases with the decrease of the collector radius and increases with the increase in the collector radius. The graph of the relationship between the collector radius and the maximum air velocity in the system is given in Figure 5. When the regression is examined, it is seen that it tends to converge. For this reason, it can be expected that the increase in air flow rate will decrease at higher collector radii and remain constant after a point. The maximum air flow rate for different collector radii can be calculated with the following equation:

$$V_m = 24.19 - 20.51e^{-0.005763R_{coll}} \quad \textbf{(16)}$$

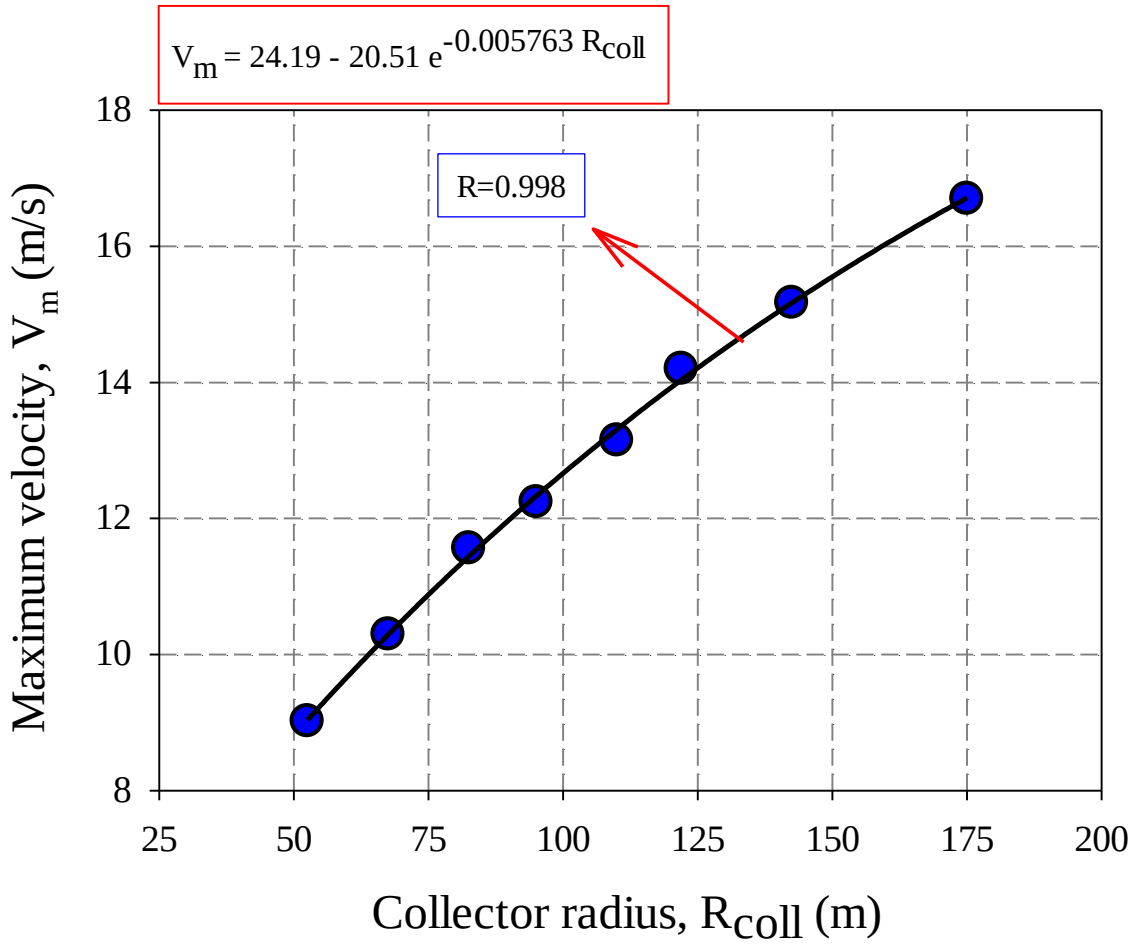

Figure 5. Variation of maximum air velocity in the system with collector radius

It is clearly understood from the CFD results that the maximum air velocity in the system increases with the collector radius. The mass flow rate is directly related to the air velocity in the system. The increase in the collector radius increases the maximum air flow rate in the system, which creates an expectation that the mass flow rate will also increase. The relationship between the collector radius and the mass flow rate is shown in Figure 6. Looking at the results, it is seen that the mass flow exhibits a similar trend to the maximum air flow rate. In this case, it is expected that the mass flow rate will increase with the increase in the collector radius. However, it can be said that the increase gradually decreases and tends to converge. The mass flow at different radii can be calculated with the following equation:

$$\dot{m} = -1831e^{-5.654\times10^{-3}R_{coll}} + 2043e^{-1.857\times10^{-13}R_{coll}} \quad \textbf{(17)}$$

There are two important parameters in the calculation of power output in SCPP systems. One is the volumetric flow and the other is the turbine pressure drop. The increase in mass flow creates the impression of a similar increase in power output. Theoretically, the increase in the energy entering the system with the increase in the collector radius results in an increase in the output of the system.

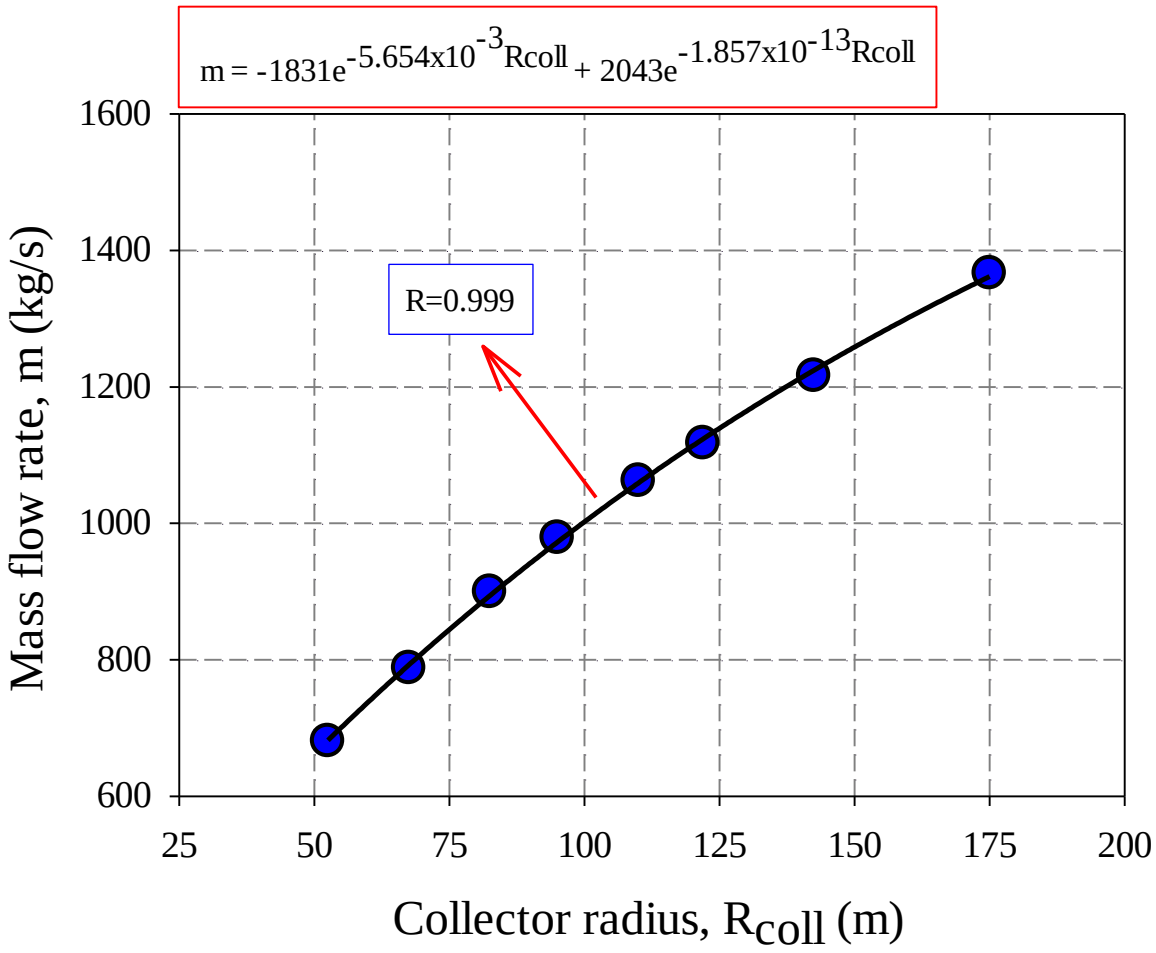

Figure 6. Variation of mass flow rate with collector radius

The relationship between the collector radius and the power output of the system is given in Figure 7. It is seen that if the collector radius of the system, which gives a power output between 55 and 60 kW with a collector radius of 122 m in the reference case, is made 175 m, the power output will approach 100 kW. When the regression is examined, it is observed that the power output increases exponentially with the collector radius. However, when evaluated together with the mass flow and maximum air flow graphs in the system, it can be considered that the power output of the system may converge at larger collector radii. For this reason, larger collector radii will be included in the calculations in future studies. The possible power outputs of different collector radii can be calculated with the following equation:

$$P_o = -12180 + 370.1R_{coll} + 1.423{R_{coll}}^2 \quad \textbf{(18)}$$

Another critical point of the researchers in the performance assessment of SCPPs is the system efficiency. Especially today, where the effective use of renewable energy sources is important, this issue is comprehensively evaluated by researchers. The efficiency of the Manzanares pilot plant is around 0.1%. It is clearly seen in the previous graph that the increase in the collector radius increases the power output of the system. However, when calculating the system efficiency according to equation (11), there is a decrease in the efficiency of the system due to the increase in the collector area in the denominator.The system efficiency graph depending on the collector radius is given in Figure 8. In addition, the efficiency can be determined by the following equation:

$$\eta = 0.1367 - 7.708 \times 10^{-4}R_{coll} + 6.81 \times 10^{-6}R_{coll} - 2.152 \times 10^{-8}R_{coll} \quad \textbf{(19)}$$

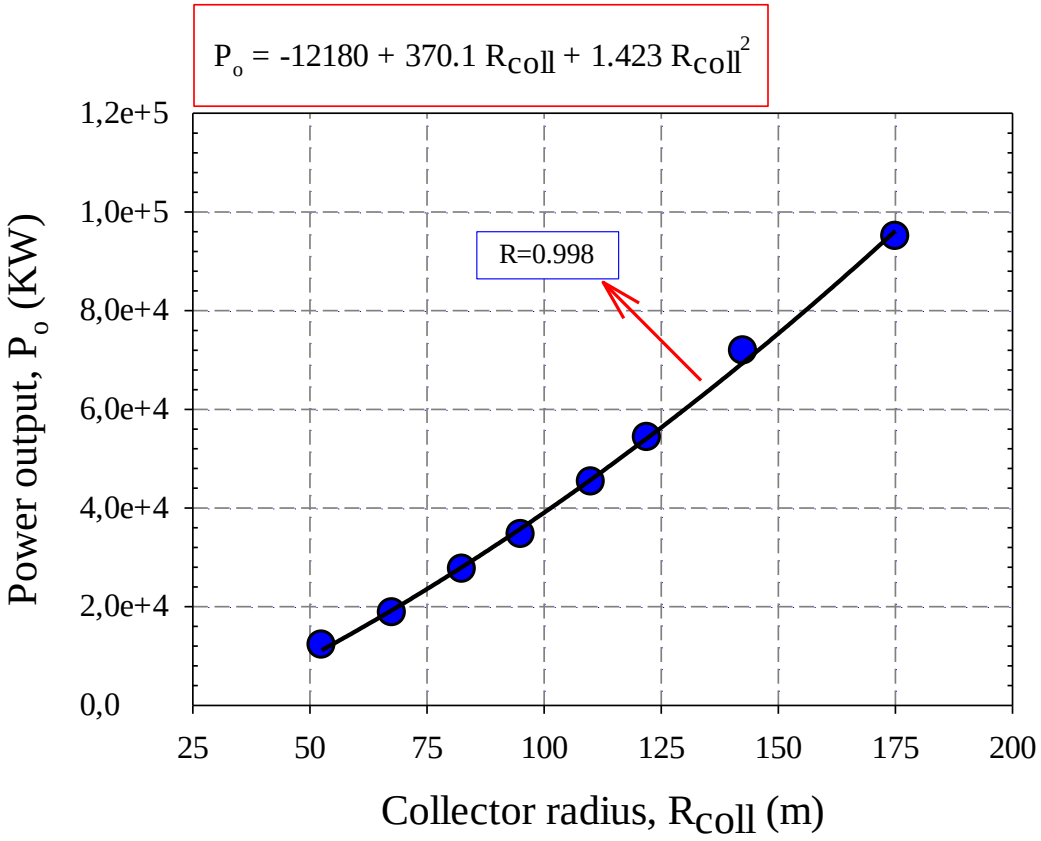

Figure 7. Power output of SCPP with different collector radius

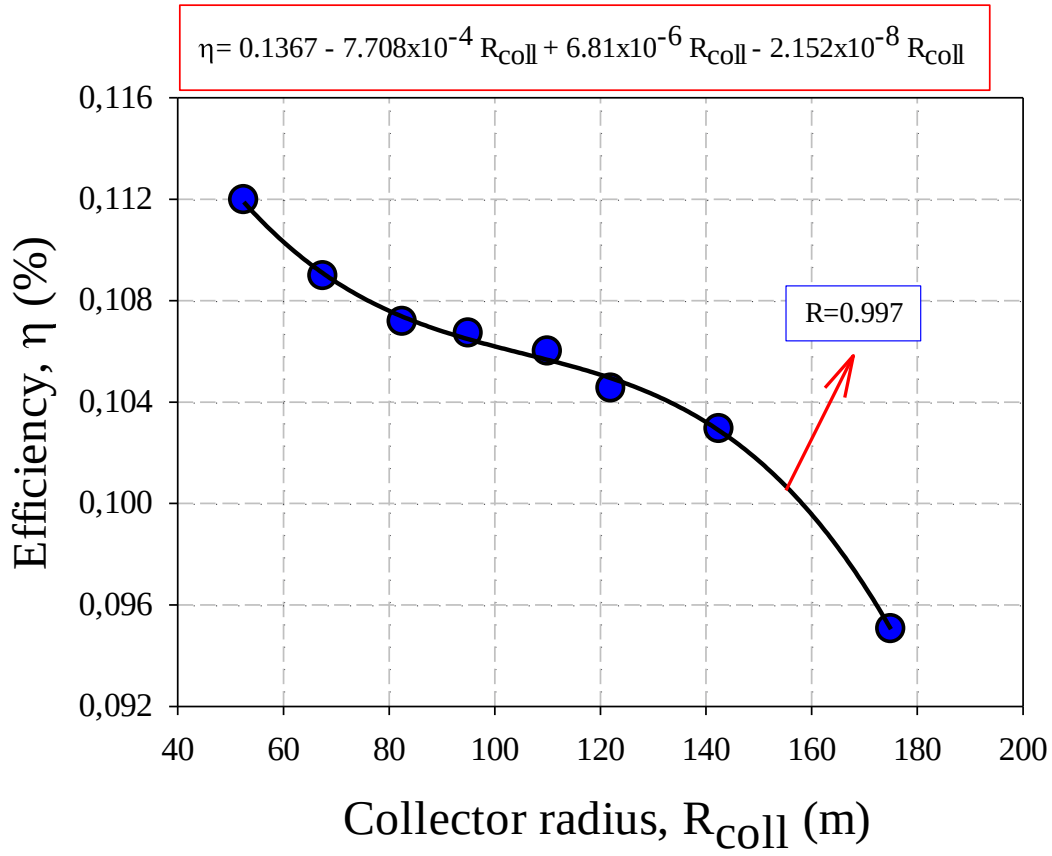

Figure 8. System efficiency of SCPP for different collector radius.

Air intake to the system takes place from the part of the collector that is open to the ambient air. This zone is called the collector input. Since the system fluid is air, transferring more air into the system can allow for greater power output. Therefore, the collector inlet height is important. This section examines how the height of the collector affects the system performance. The collector radius is kept constant at 122 m and the collector height is changed between 1.1-4 m and its effects on the system are interpreted. The temperature distribution in the system is given in Figure 9 for 3 different collector heights. When the contours are compared, it is understood that while the maximum air temperature in the system is 349.462 K in the reference case, the maximum temperature drops to 349.099 K when the collector height is reduced to 1.1 m. This is because reducing the collector height increases the airflow rate through the system. The increase in the velocity of the system air causes the system air under the collector to be less exposed to the effects of heat transfer. This results in a lower system air temperature. Increasing the collector height has the opposite effect. The velocity of the system air decreases with the increase in the collector height. In this case, the temperature of the system air is expected to increase. The contours support this notion.

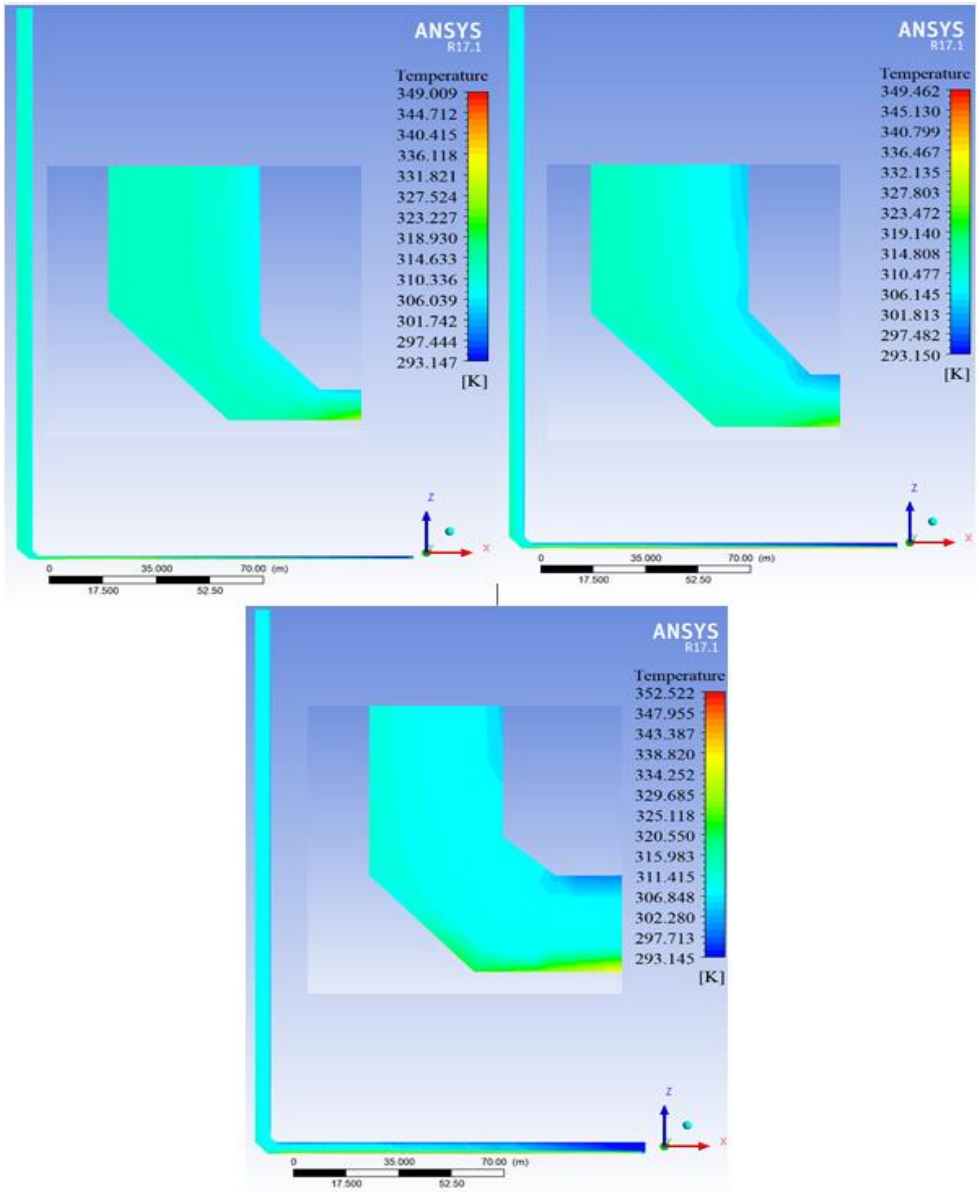

Figure 9. Temperature contours for 1.1, 1.85 and 4 m collector height

It is concluded that the increase in the height of the collector, which is the part that feeds the system, will support the inclusion of more air into the system. This situation is not similar for air flow rate. An increase in collector height allows more air to enter the system, but the reverse is true for air flow rate. As the collector height increases, the air flow rate decreases. The relationship between the collector height and the maximum air flow rate is given in Figure 10. It is seen that the maximum air velocity, which is approximately 14.2 m/s in the reference case, approaches 17 m/s with the decrease of the collector height. As the collector height increases, it is understood that the air flow rate decreases but tends to converge. The maximum air velocities for different collector heights can be found with the following equation:

$$V_m = 13.98 - 103.3e^{-3.29H_{coll}} \quad \textbf{(20)}$$

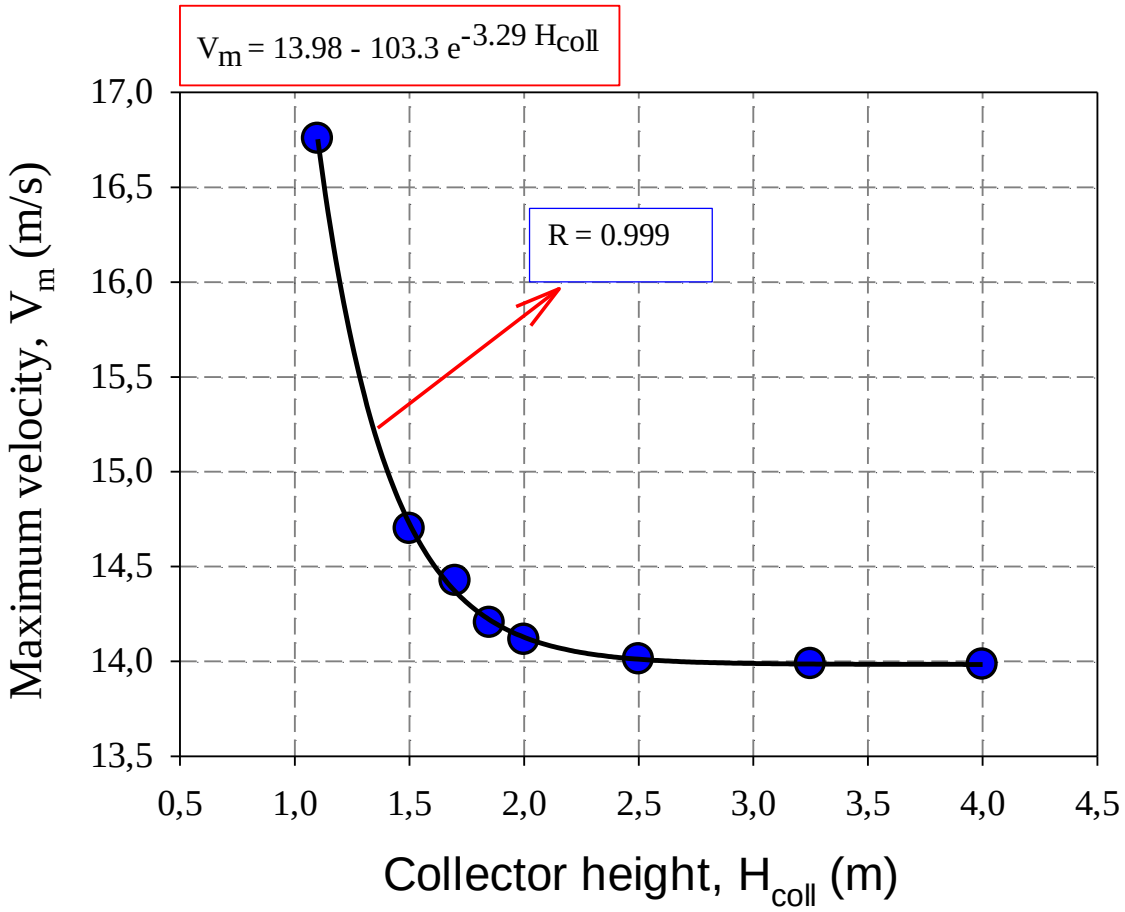

Figure 10. Maximum air velocity for different collector heights

With the increase in the collector height, more air is included in the system. In this case, although the energy entering the system is constant, its temperature is expected to decrease as more air enters the system. The relationship between the collector height and the temperature rise in the collector is given in Figure 11. As expected, increasing the collector height reduces the temperature rise in the collector. Here, what is meant by the temperature increase in the collector is how much the temperature of the air entering the collector increases until it leaves the collector. The following equation can be used for the temperature rise that will occur at different collector heights:

$$\Delta T = 217.4e^{-4.667H_{coll}} + 17.71e^{0.04262H_{coll}} \quad \textbf{(21)}$$

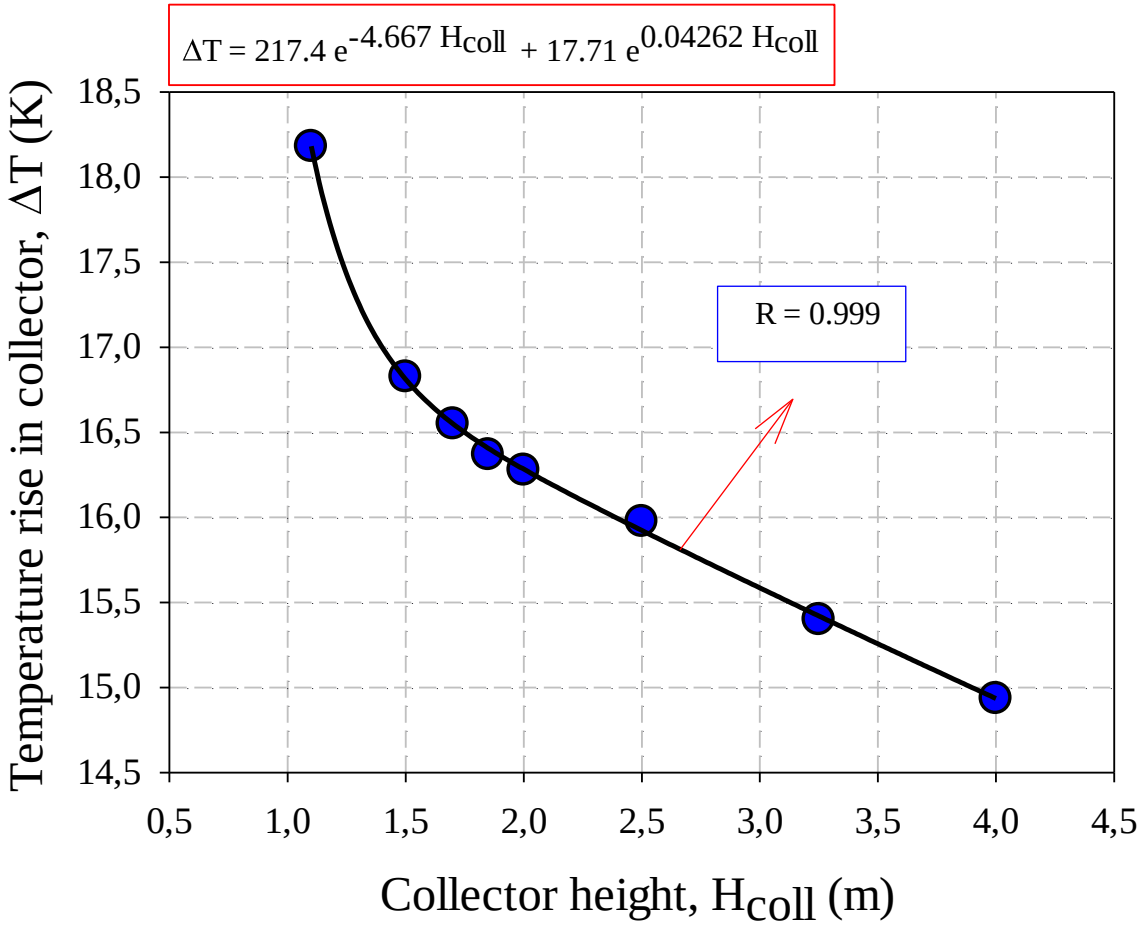

Figure 11. Temperature rise in collector for different collector heights

It is seen in the previous graph that the collector height reduces the maximum air velocity in the system. However, the increased airflow area with collector height compensates for the reduction in velocity. Thus, the mass flow rate of the system increases with the collector height. Figure 12 shows the relationship between the collector height and the mass flow rate of the system. It is seen that the mass flow rate of the facility, which is approximately 1100 kg/s with a collector height of 1.85 in the reference case, decreases below 1000 kg/s with the reduction of the collector height. With the increase in the collector height, the mass flow rate of the system increases, but this increase is not even 15%. The mass flow rate at any value of collector height can be calculated by the equation:

$$\dot{m} = 1143 - 2083e^{-2.422H_{coll}} \quad \textbf{(22)}$$

When the effect of the collector height on the power output is examined, it is expected that the power output will decrease considering the decrease in the maximum air velocity and the low increase in the mass flow rate. The power output graph with the collector height is given in Figure 13. It can be seen from the graph that the power output, which is approximately 55 kW in the reference geometry, can be increased by 10% by decreasing the collector height. It also shows that keeping the collector height low would be ideal for higher power output. It is seen that the power output tends to stabilize, approaching 50 kW with the collector height. The power output of the system for different collector heights can be given by the following equation:

$$P_o = 77600 - 17050H_{coll} + 2738{H_{coll}}^2 - 64.37{H_{coll}}^3 \quad \textbf{(23)}$$

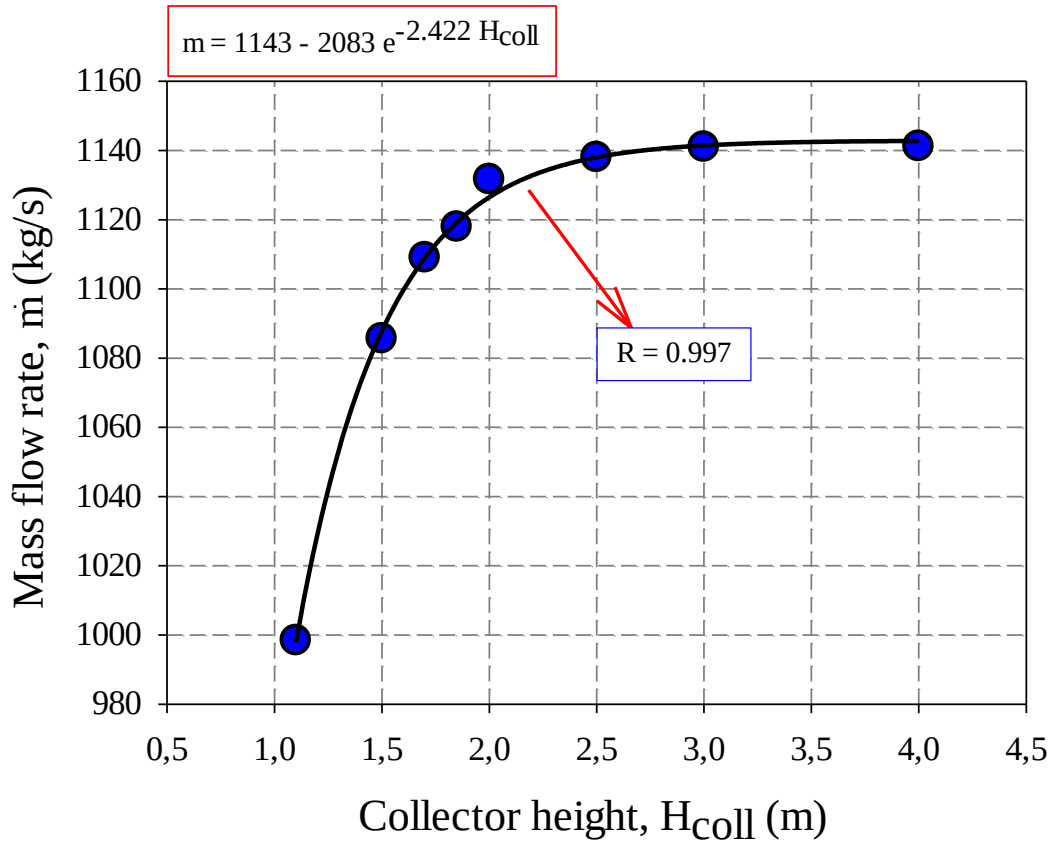

Figure 12. Mass flow rate for different collector heights

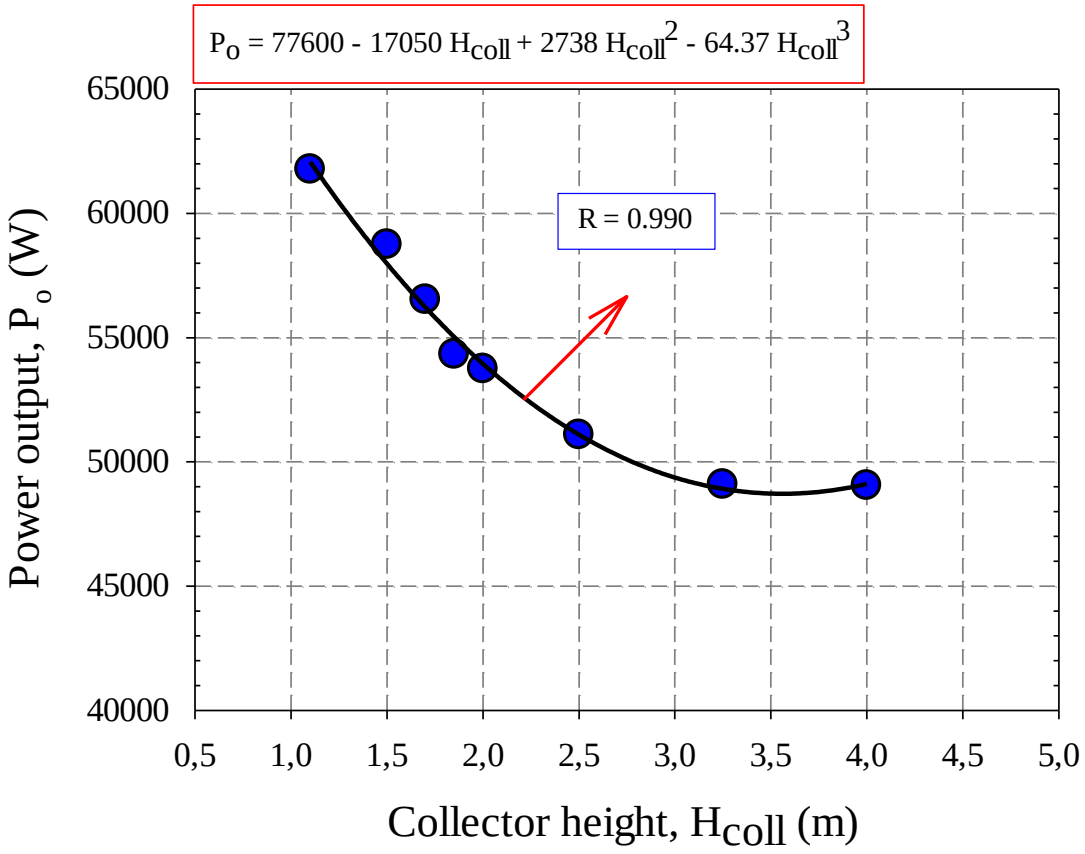

Figure 13. Power output for different collector heights

The efficiencies of SCPP systems are in parallel with their power outputs. When the energy input to the system is constant, an increase in power output causes an increase in efficiency, and a decrease in power output causes a decrease in efficiency. Since the change in the collector height does not change the collector area, it does not change the energy entering the system. In this case, the efficiency of the system is expected to show a similar trend to the power output. It is seen that the system efficiency, which is more than 0.1% in the reference geometry, decreases below 0.1% with the increase in the collector height. The graph of the efficiency of the system depending on the collector height is in Figure 14. The efficiency of the system at different collector heights can be calculated with the following equation:

$$\eta = 0.1673 - 0.07499(1 - e^{-0.8954 H_{coll}}) \quad \textbf{(24)}$$

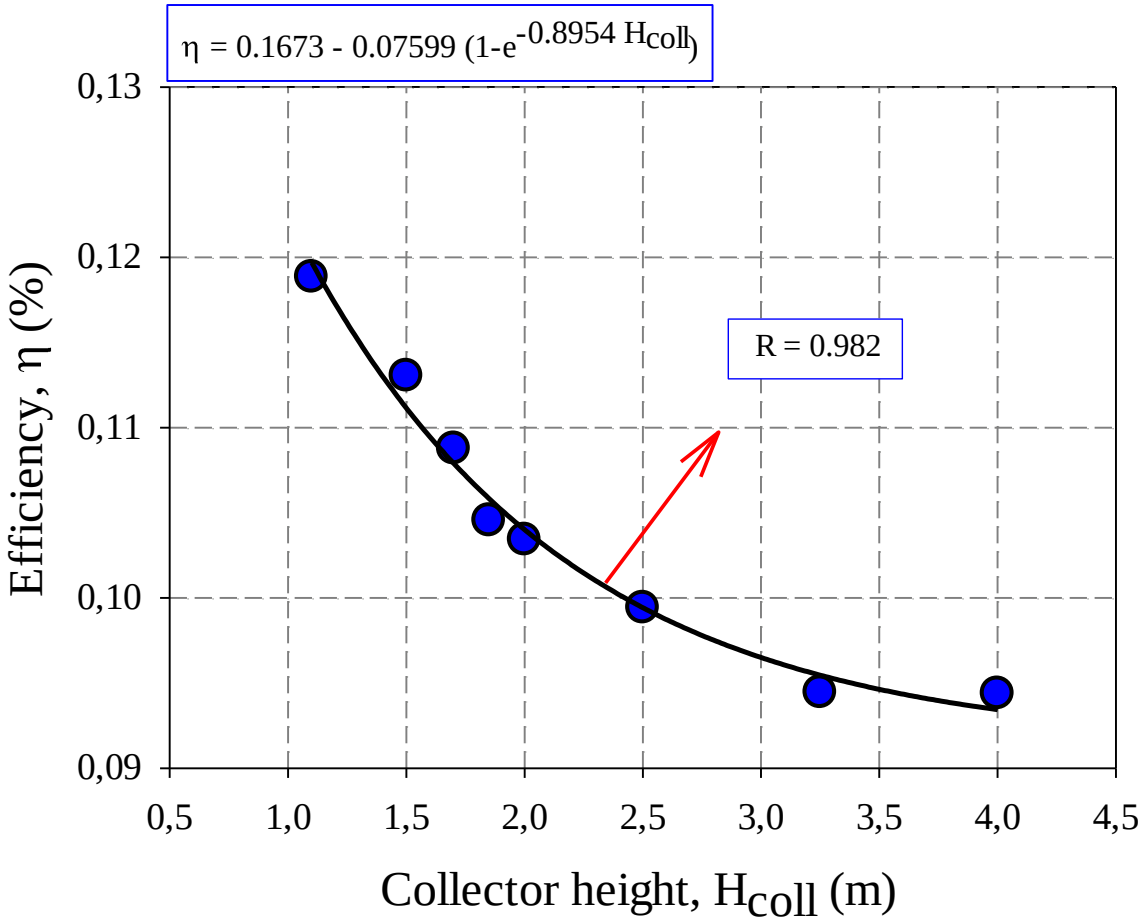

Figure 14. System efficiency for different collector heights

4. Conclusion

The influence of collector radius and height on the performance figures of Manzanares pilot plant is examined. A 3D CFD model is created with reference to the pilot plant characteristics. In the CFD model, the solar radiation discrete ordinates (DO) is included in the system with the solar ray tracing algorithm. In addition, for the turbulence model, the RNG k-ε turbulence model is included in the analysis considering the greenhouse effect. All simulations are carried out at a constant 1000 W/m^2 solar intensity and 293.15 K ambient temperature. First, the collector radius is changed between 52.5-175 m, keeping the collector height constant at 1.85 m. Then the collector radius is fixed at 122 m and the collector height is changed between 1.1-4 m.

When the simulations are evaluated, the following conclusions can be drawn:

• The CFD model shows good agreement with the experimental data under stable climatic conditions. The power output, which is 54.3 kW at 1000 W/m^2 radiation intensity, is approximately 50 kW in experimental measurements.

• There is a linear relationship between the collector radius and the temperature rise in the collector.

• Mass flow rate and maximum velocity tend to increase with the collector radius. However, both show to converge after a certain value.

• The power output increases exponentially with the collector radius. The power output, which is 54.3 kW at 122 m collector radius, increases by 75% to 95 kW with the 175 m collector radius.

• The efficiency of the system decreases with the increase in the collector radius. This is because the collector area increases with increasing radius. The efficiency of the system becomes 0.095% at a collector radius of 175 m.

• Collector height reduces the performance of the system. Reducing the collector height for the pilot plant to 1.1 m can increase the power output by up to 13% to 61.77 kW.

When the results are evaluated, the collector radius and height are the parameters that should be evaluated in a wide range of dimensions. The dual effects of collector height and collector radius will be combined in future studies with different design aspects.

References

Abdelmohimen, M.A.H. Algarni, S.A. (2018). Numerical investigation of solar chimney power plants performance for Saudi Arabia weather conditions. *Sustainable Cities and Society*, 38, 1-8. DOI: https://doi.org/10.1016/j.scs.2017.12.013

Ahirwar, M. J., Sharma, P. (2019). Analyzing the effect of solar chimney power plant by varying chimney height, collector slope and chimney diverging angle. *International Journal of Innovative Research in Technology*, 6(7), 213-219.

Al Alawin, A., Badran, O., Awad, A., Abdelhadi, Y., Al-Mofleh, A. (2012). Feasibility study of a solar chimney power plant in Jordan. *Applied Solar Energy*, 48(4), 260-265. DOI: https://doi.org/10.3103/S0003701X12040020

Ansys Inc, 2016. ANSYS Fluent 16 Theory Guide.

Ayadi, A., Driss, Z., Bouabidi, A., Nasraoui, H., Bsisa, M., Abid, M.S. (2018). A computational and an experimental study on the effect of the chimney height on the thermal characteristics of a solar chimney power plant. *Proceedings of the Institution of Mechanical Engineers, Part E: Journal of Process Mechanical Engineering*, 232(4), 503-516. DOI: https://doi.org/10.1177%2F0954408917719776

Bouabidi, A., Ayadi, A., Nasraoui, H., Driss, Z., Abid, M.S. (2018). Study of solar chimney in Tunisia: Effect of the chimney configurations on the local flow characteristics. *Energy and Buildings*, 169, 27-38. DOI: https://doi.org/10.1016/j.enbuild.2018.01.049

Cuce, E. and Bali, T. (2009). Variation of cell parameters of a p-Si PV cell with different solar irradiances and cell temperatures in humid climates. *Fourth International Exergy, Energy and Environment Symposium. 19-23 April 2009, Sharjah, United Arab Emirates*.

Cuce, E., Cuce, P.M. (2019a). Performance assessment of solar chimneys: Part 1 – Impact of chimney height on power output. *Energy Research Journal*, 10, 11-19.

Cuce, E., Cuce, P.M. (2019b). Performance assessment energy research journal of solar chimneys: Part 2 – Impacts of slenderness

value and collector slope on power output. *Energy Research Journal*, 10, 20-26.

Cuce, E., Cuce, P.M., Sen, H. (2020a). A thorough performance assessment of solar chimney power plants: Case study for Manzanares. *Cleaner Engineering and Technology*, 1, 100026. DOI: https://doi.org/10.1016/j.clet.2020.100026

Cuce, E., Sen, H., Cuce, P.M. (2020b). Numerical performance modelling of solar chimney power plants: Influence of chimney height for a pilot plant in Manzanares, Spain. *Sustainable Energy Technologies and Assessments*, 39, 100704. DOI: https://doi.org/10.1016/j.seta.2020.100704

Cuce, P.M., Cuce, E., Sen, H. (2020c). Improving electricity production in solar chimney power plants with sloping ground design: an extensive CFD research. *Journal of Solar Energy Research Updates*, *7*(1), 122-131. DOI: http://dx.doi.org/10.31875/2410-2199.2020.07.9

Cuce, E., Saxena, A., Cuce, P.M., Sen, H., Guo, S., Sudhakar, K. (2021a). Performance assessment of solar chimney power plants with the impacts of divergent and convergent chimney geometry. *International Journal of Low-Carbon Technologies*. DOI: https://doi.org/10.1093/ijlct/ctaa097

Cuce, E., Cuce, P.M., Sen, H., Sudhakar, K., Berardi, U., Serencam, U. (2021b). Impacts of ground slope on main performance figures of solar chimney power plants: A comprehensive CFD research with experimental validation. *International Journal of Photoenergy*, *2021*. DOI: https://doi.org/10.1155/2021/6612222

Dai, Y.J., Huang, H.B., Wang, R.Z. (2003). Case study of solar chimney power plants in Northwestern regions of China. *Renewable Energy*, 28(8), 1295-1304. DOI: https://doi.org/10.1016/S0960-1481(02)00227-6

Daimallah, A., Lebbi, M., Lounici, M. S., Boutina, L. (2020). Effect of thermal collector height and radius on hydrodynamic flow control in small solar chimney. *Journal of Advanced Research in Fluid Mechanics and Thermal Sciences*, 71(2), 10-25. DOI: https://doi.org/10.37934/arfmts.71.2.1025

Das, P., Chandramohan, V.P. (2020). 3D numerical study on estimating flow and performance parameters of solar updraft tower (SUT) plant: Impact of divergent angle of chimney, ambient temperature, solar flux and turbine efficiency. *Journal of Cleaner Production*, 256, 120353. DOI: https://doi.org/10.1016/j.jclepro.2020.120353

Dewangan, S.K. (2021). Effect of collector roof cum chimney divergence and exhaust fan on solar chimney power plant performance. *International Journal of Energy and Environmental Engineering*, 1-18. DOI: https://doi.org/10.1007/s40095-021-00426-9

Dhahri, A., Omri, A. (2013). A review of solar chimney power generation technology. *International Journal of Engineering and Advanced Technology*, *2*(3), 1-17.

Dhahri, A., Omri, A., Orfi, J. (2014). Numerical study of a solar chimney power plant. *Research Journal of Applied Sciences, Engineering and Technology*, *8*(18), 1953-1965. DOI: https://dpi.org/10.19026/rjaset.8.1187

dos Santos Bernardes, M.A., Von Backström, T.W., Kröger, D.G. (2009). Analysis of some available heat transfer coefficients applicable to solar chimney power plant collectors. *Solar Energy*, 83(2), 264-275. DOI: https://doi.org/10.1016/j.solener.2008.07.019

Guo, P.H., Li, J.Y., Wang, Y. (2014). Numerical simulations of solar chimney power plant with radiation model. *Renewable energy*, 62, 24-30. DOI: https://doi.org/10.1016/j.renene.2013.06.039

Haaf, W., Friedrich, K., Mayr, G., Schlaich, J. (1983). Solar chimneys part I: principle and construction of the pilot plant in Manzanares. *International Journal of Solar*

Energy, *2*(1), 3-20. DOI: https://doi.org/10.1080/01425918308909911

Haaf, W. (1984). Solar chimneys: part ii: preliminary test results from the Manzanares pilot plant. *International Journal of Sustainable Energy*, *2*(2), 141-161. DOI: https://doi.org/10.1080/01425918408909921

Hassan, A., Ali, M., Waqas, A. (2018). Numerical investigation on performance of solar chimney power plant by varying collector slope and chimney diverging angle. *Energy*, 142, 411-425. DOI: https://doi.org/10.1016/j.energy.2017.10.047

Hoseini, H., Mehdipour, R. (2018). Evaluation of solar-chimney power plants with multiple-angle collectors. *Journal of Computational & Applied Research in Mechanical Engineering (JCARME)*, 8(1), 85-96. DOI: https://dx.doi.org/10.22061/jcarme.2017.2282.1213

Hu, S., Leung, D. Y., Chan, J. C. (2017). Impact of the geometry of divergent chimneys on the power output of a solar chimney power plant. *Energy*, 120, 1-11. DOI: https://doi.org/10.1016/j.energy.2016.12.098

Kashiwa, B.A., Kashiwa, C.B. (2008). The solar cyclone: A solar chimney for harvesting atmospheric water. *Energy*, 33(2), 331-339. DOI: https://doi.org/10.1016/j.energy.2007.06.003

Keshari, S. R., Chandramohan, V. P., Das, P. (2021). A 3D numerical study to evaluate optimum collector inclination angle of Manzanares solar updraft tower power plant. *Solar Energy*, 226, 455-467. DOI: https://doi.org/10.1016/j.solener.2021.08.062

Li, J. Y., Guo, P. H., Wang, Y. (2012). Effects of collector radius and chimney height on power output of a solar chimney power plant with turbines. *Renewable Energy*, 47, 21-28. DOI: https://doi.org/10.1016/j.renene.2012.03.018

Mullett, L.B. (1987). The solar chimney-overall efficiency, design and performance. *International journal of ambient energy*, *8*(1), 35-40. DOI: https://doi.org/10.1080/01430750.1987.9675512

Nasraoui, H., Driss, Z., Kchaou, H. (2020). Effect of the chimney design on the thermal characteristics in solar chimney power plant. *Journal of Thermal Analysis and Calorimetry*, 140(6), 2721-2732. DOI: https://doi.org/10.1007/s10973-019-09037-3

Nizetic, S., Ninic, N., Klarin, B. (2008). Analysis and feasibility of implementing solar chimney power plants in the Mediterranean region. *Energy*, 33(11), 1680-1690. DOI: https://doi.org/10.1016/j.energy.2008.05.012

Pasumarthi, N., Sherif, S.A. (1998a). Experimental and theoretical performance of a demonstration solar chimney model-Part I: mathematical model development. *International Journal of Energy Research*, 22(3), 277-288. DOI:https://doi.org/10.1002/(SICI)1099-114X(19980310)22:3<277::AID-R380>3.0.CO;2-R

Pasumarthi, N., Sherif, S.A. (1998b). Experimental and theoretical performance of a demonstration solar chimney model-Part II: experimental and theoretical results and economic analysis. *International journal of energy research*, 22(5), 443-461. DOI: https://doi.org/10.1002/(SICI)1099-114X(199804)22:5<443::AID-ER381>3.0.CO;2-V

Schlaich, J., Bergermann, R., Schier W., Weinrebe, G. (2005). Design of commercial solar updraft tower systems utilization of solar induced convective flows for power generation. *J Sol Energy Eng*, 127(1), 117–24. DOI: https://doi.org/10.1115/1.1823493

Sen, H., Cuce, E. (2020). Dynamic pressure distributions in solar chimney power plants: A numerical research for the pilot plant in Manzanares, Spain. *WSSET Newsletter*, 12(1), 2-2.

Setareh, M. (2021). Comprehensive mathematical study on solar chimney powerplant. *Renewable Energy*, 175, 470-485. DOI: https://doi.org/10.1016/j.renene.2021.05.017

Shahi, D.V.V., Gupta, M.A., Nayak, M.V.S. (2018). CFD Analysis of solar chimney wind power plant by Ansys Fluent. *Int J Technol Res Eng*, *5*(9), 3746-3751.

Tayebi, T., Djezzar, M., Gouidmi, H. (2018). 3D numerical study of flow in a solar chimney power plant system. *Sciences & Technology*, *3*(1), 17-20.

Toghraie, D., Karami, A., Afrand, M., Karimipour, A. (2018). Effects of geometric parameters on the performance of solar chimney power plants. *Energy*, *162*, 1052-1061. DOI: https://doi.org/10.1016/j.energy.2018.08.086

Xu, Y., Zhou, X. (2018). Performance of divergent-chimney solar power plants. *Solar Energy*, 170, 379-387. DOI: https://doi.org/10.1016/j.solener.2018.05.06

Yapıcı, E.Ö., Ayli, E., Nsaif, O. (2020). Numerical investigation on the performance of a small scale solar chimney power plant for different geometrical parameters. *Journal of Cleaner Production*, 276, 122908. DOI: https://doi.org/10.1016/j.jclepro.2020.122908

Zandian, A., Ashjaee, M. (2013.) The thermal efficiency improvement of a steam Rankine cycle by innovative design of a hybrid cooling tower and a solar chimney concept. Renewable Energy, 51, 465-473. DOI: https://doi.org/10.1016/j.renene.2012.09.051

Zhou, X., Yang, J., Xiao, B., Hou, G. (2007) Experimental study of temperature field in a solar chimney power setup. *Applied Thermal Engineering*, 27(11-12), 2044-2050. DOI: https://doi.org/10.1016/j.applthermaleng.2006.12.007

Zhou, X., Yang, J., Xiao, B., Hou, G., Xing, F. (2009). Analysis of chimney height for solar chimney power plant. *Applied Thermal Engineering*, 29(1), 178-185. DOI: https://doi.org/10.1016/j.applthermaleng.2008.02.014